PAPER • OPEN ACCESS

Effect of multi-step annealing with different heating rates on magnetic properties of Fe-Si-B-P-Cu nano-crystalline alloy

To cite this article: Ziyan Hao *et al* 2022 *Mater. Res. Express* **9** 126102

View the article online for updates and enhancements.

Materials Research Express

Effect of multi-step annealing with different heating rates on magnetic properties of Fe-Si-B-P-Cu nano-crystalline alloy

Ziyan Hao[1], Linzhuo Wei[1,2], Yuanfei Cai[3], Yaocen Wang[1,2,*] ⓘ, Mingliang Xiang[3], Fang Zhao[4], Yan Zhang[3,*], Nikolai S Perov[5] and Chongde Cao[1,2,*]

[1] School of Physical Science and Technology, Northwestern Polytechnical University, Xi'an 710072, People's Republic of China
[2] Research and Development Institute of Northwestern Polytechnical University in Shenzhen, Shenzhen 518057, People's Republic of China
[3] Ningbo Institute of Materials Technology and Engineering, Chinese Academy of Sciences, Ningbo 315201, People's Republic of China
[4] TIZ Advanced Alloy Technology Co., Ltd, Quanzhou 362000, People's Republic of China
[5] Faculty of Physics, Lomonosov Moscow State University, Moscow 119991, Russia
*   Authors to whom any correspondence should be addressed.

E-mail: wangyc@nwpu.edu.cn, yzhang@nimte.ac.cn and caocd@nwpu.edu.cn

Keywords: nano-crystalline, thermal stability, soft magnetic, coercivity, multi-step heating

Abstract

The crystallization behaviors of $Fe_{83}Si_4B_8P_{4.3}Cu_{0.7}$ amorphous alloy with different heating rates and magnetic softness of annealed alloys have been widely studied. The rapid heating significantly helped with the decrease of coercivity for annealed samples compared with that for slow heating. It is found that the peak temperature (T_{p1}) of the first crystallization stage in DSC curves is a critical temperature parameter to distinguish the nucleation and growth processes of α-Fe phase. When the temperature at a constant heating rate is beyond the T_{p1}, the nucleation process should be almost finished. The necessary temperature range of high heating rate ($400\,K\,min^{-1}$) for the improvement of magnetic softness has been determined from 650 K to 740 K through multi-step annealing with different heating rates. The shortened temperature window of rapid heating and partial rapid heating may simplify and improve the annealing process of high-performance soft magnetic materials in industry. The multi-step annealing with various heating rates also provides a promising strategy for the investigation of crystallization behaviors of amorphous alloys.

1. Introduction

With high saturation flux density (B_s) and low coercivity (H_c) along with high effective permeability (μ_e), soft magnetic materials have played important roles in many fields, such as electrical transformers, inductors and automotive sectors. Up to now, some traditional soft magnetic materials have been well developed, such as Si-steel, ferrites and metallic glasses (MGs) [1–3]. However, the magnetic properties of these materials seem to meet their ceilings to a certain degree. For example, the B_s of Mn-Zn ferrites are always found below 0.5 T, which is insufficient for many applications [2]. Despite the high B_s of 1.7–2.0 T, the μ_e of Si-steels are limited in the range of 2,000–6,000 at 1 kHz [4]. Fe-based MGs (i.e. Fe-P-C and Fe-Si-B-P) exhibit relatively high μ_e around 4,000–11,000 at 1 kHz but still insufficient B_s of 1.5–1.6 T [5, 6]. Fe-based nano-crystalline materials, formed from amorphous precursors through the delicate annealing, have been regarded as the promising candidate of traditional counterparts due to their excellent soft magnetic properties, especially high B_s and large μ_e [7–10].

Since the first report of Fe-Si-B-Nb-Cu nano-crystalline alloys by Yoshizawa *et al* [11], much attention has been paid to the further development of compositions and annealing conditions to overcome the insufficient B_s of 1.2 T. Fe-Zr-B nano-crystalline alloys with high B_s of 1.70 T were developed by Suzuki *et al* [12]. In addition to the magnetic properties after annealing, the preparation environment of amorphous precursors also should be considered. The inert gas atmosphere is commonly imperative for Zr-containing precursors during melt-spinning. On the other hand, the large-size transition metals (TMs, such as Nb, Zr and W) would also deteriorate the B_s of nano-crystalline alloys, although they could prevent the coarsening of α-Fe gains and bring a better
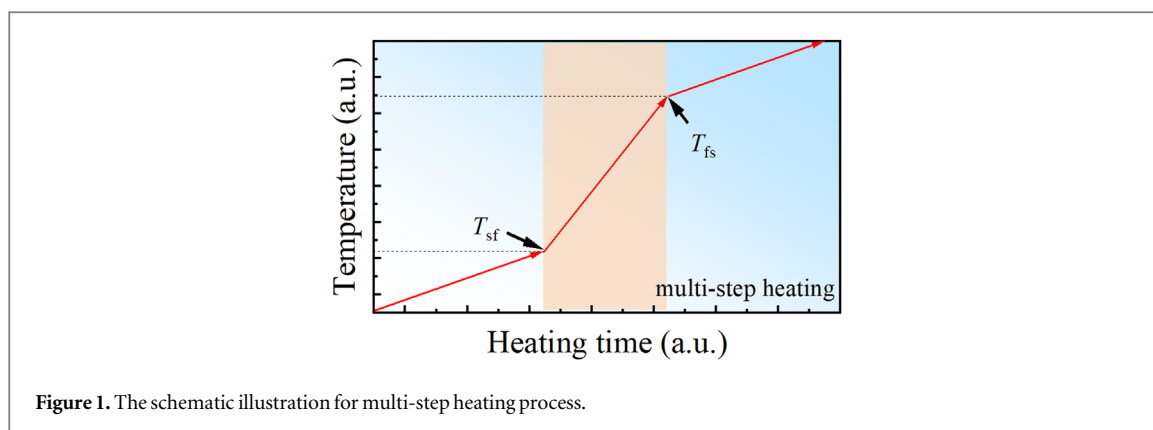
Figure 1. The schematic illustration for multi-step heating process.

magnetic softness [13, 14]. Thus, the attempts of TMs-free nano-crystalline alloys with sufficient magnetic softness are urgent to fill in gaps for related fields.

Makino et al [15] have reported that both the low H_c below 10 A m^{-1} and a high B_s of 1.9 T could be obtained in Fe-Si-B-P-Cu alloys through 400 K min^{-1} heating, with the features of P addition and avoiding the addition of TMs. This alloy system has been regarded as the significantly promising soft magnetic materials. In fact, Fe-B nano-crystalline alloys with excellent magnetic properties and ultra-fine α-Fe grains could also be fabricated by ultra-rapid annealing [16]. For most Fe-based nano-crystalline alloys, the high heating rate seems always effective in decreasing the coercivity of annealed samples [16–18]. But due to the severe brittleness of annealed ribbons, soft magnetic nano-crystalline alloys in most applications need to be stacked in multi-layers before the annealing process. It is difficult to control the heat treatment process when the high heating rate is necessary for ultra-fine structures of annealed alloys [19, 20]. For further solving the problems in high-performance nano-crystalline alloys, the mechanism of heating rate for decreasing the coercivity has been investigated to develop new compositions independent on the high heating rate for realizing controllable heating in industry [20]. However, the effect of heating rates on nucleation and growth processes of α-Fe along with the effective temperature window of rapid heating for Fe-based nano-crystalline materials are still unclear [20, 21].

In this study, the multi-step heating during the annealing was applied to investigate the effect of magnetic softness on heating rates for Fe$_{83}$Si$_4$B$_8$P$_{4.3}$Cu$_{0.7}$ nano-crystalline alloys. The nucleation and growth processes have been distinguished according to the thermal behaviors of as-spun alloy and coercivity evolution of annealed samples. The necessary temperature window of high heating rate has been determined through multi-step heating. Partial rapid heating also made a fine effect on the decrease of coercivity for annealed samples. To a certain extent, the shortened temperature range of high heating rate could improve the controllability of heat treatment process for fabricating high-performance materials in industry.

2. Experimental procedures

Fe$_{83}$Si$_4$B$_8$P$_{4.3}$Cu$_{0.7}$ ingot with the weight of 30 g was prepared through high-frequency induction melting in argon atmosphere with high pure Fe (99.99%), Si (99.99%), Cu (99.99%), B (99.9%) and phosphides (99.7% Fe$_3$P). Then the ingot was cut into small pieces for preparing ribbons. The as-spun ribbons with the thickness of about 20 μm and width of about 1.5 mm were produced through the single roller melt-spinning technology with a linear velocity of about 40 m s^{-1}. The annealing processes of as-spun samples were carried out by an infra-red oven with the flowing argon atmosphere against oxidation, which could provide a series of heating rates in this study. First, the annealing processes with constant heating rates of 400 K min^{-1} and 10 K min^{-1} were applied to investigate the dependence of coercivity on the annealing temperature. Then, the two-step heating of slow-fast heating process with the switching temperature T_{sf} and the reversal fast-slow one with T_{fs} were carried out to provide references for the investigation of effective temperature window of rapid heating for decreasing the coercivity of annealed samples. According to the coercivity evolution of samples processed through two-step heating, the multi-step heating was designed and the schematic illustration is shown in figure 1.

The structures of as-spun and annealed samples were identified with an x-ray diffractometer (XRD, Shimadzu XRD-700) equipped with Cu target. The phases in XRD patterns of annealed samples were distinguished by Jade software. A differential scanning calorimetry (DSC, NETZSCH 404C) was used for investigating thermal behaviors for as-spun samples at the heating rates of 10, 20, 30 and 40 K min^{-1}. The coercivity values of as-spun and annealed samples were measured through a DC B-H curve tracer (Linkjoin MATS-2010SD, open flux configuration) mainly under a maximum field of 800 A m^{-1} or a larger field of 4000 A m^{-1} if necessary.

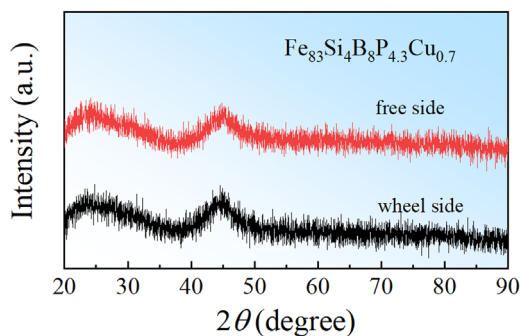**Figure 2.** XRD patterns of as-spun $Fe_{83}Si_4B_8P_{4.3}Cu_{0.7}$ alloy from the free side and wheel side.

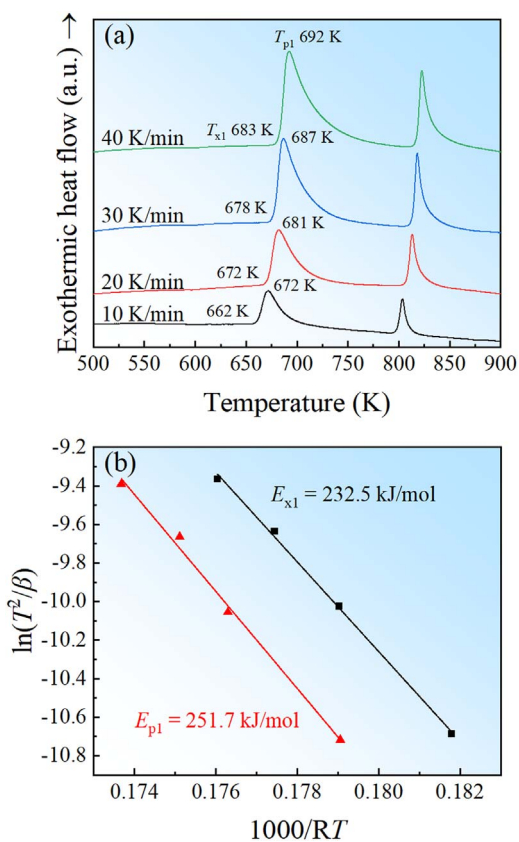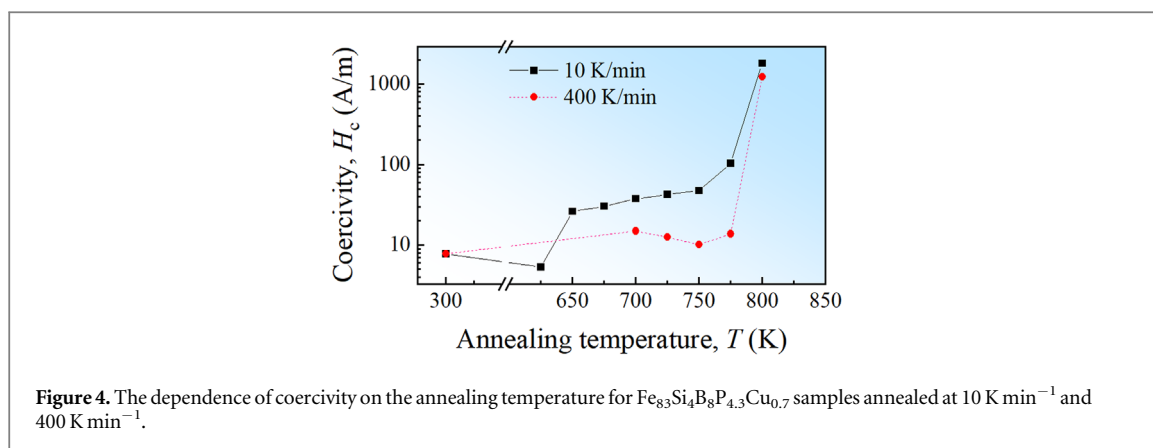**Figure 3.** DSC curves at the heating rates of 10, 20, 30, 40 K min^{-1} (a) and Kissinger fitting curves (b) for $Fe_{83}Si_4B_8P_{4.3}Cu_{0.7}$ amorphous alloy. T_{x1} and T_{p1} are the onset and peak temperatures of the first stage. β is the heating rate and R represents the universal gas constant. E_{x1} and E_{p1} are the activation energies of crystallization corresponding to T_{x1} and T_{p1}, respectively.

3. Results

3.1. Structure and thermal properties of as-spun alloy

The XRD patterns of as-spun $Fe_{83}Si_4B_8P_{4.3}Cu_{0.7}$ alloy from the free side and wheel side are shown in figure 2. Only the broad peak instead of any crystallized diffraction peaks could be observed, indicating the as-spun ribbons are completely amorphous.

For understanding the thermal behaviors of as-spun $Fe_{83}Si_4B_8P_{4.3}Cu_{0.7}$ alloy, DSC curves are measured at various heating rates of 10, 20, 30 and 40 K min^{-1} as exhibited in figure 3(a). Two stages of crystallization could be found in DSC curves. Generally, the former stage is corresponding to the precipitation of α-Fe phase and the latter one is mainly attributed to the formation of compounds (i.e. $Fe_3(B, P)$) [12, 13, 15]. The characteristic temperatures of the first stage, including the onset crystallization temperature (T_{x1}) and the peak temperature (T_{p1}), increases with the heating rate rising from 10 K min^{-1} to 40 K min^{-1}. The T_{x1} increases from 662 K to 683 K whereas the T_{p1} varies from 672 K to 692 K.

Figure 4. The dependence of coercivity on the annealing temperature for $Fe_{83}Si_4B_8P_{4.3}Cu_{0.7}$ samples annealed at $10\,K\,min^{-1}$ and $400\,K\,min^{-1}$.

To assess the thermal stability of amorphous $Fe_{83}Si_4B_8P_{4.3}Cu_{0.7}$ alloy, the crystallization activation energy E_a (i.e. E_x and E_p) has been estimated using Kissinger function [22].

$$\ln\frac{\beta}{T^2} = -\frac{E_a}{RT} + const \tag{1}$$

where β is the heating rate, T is the onset crystallization temperature for E_x or the peak temperature for E_p and R represents the universal gas constant. The appearance of compounds in the latter crystallization stage is always found to significantly deteriorate the magnetic softness of samples after annealing in previous literature [12, 13, 15]. Thus, the former stage has been mainly discussed in the following part. Based on the linear fitting of the $\ln(\beta/T^2)$ and $-1000/(RT)$ related to T_{x1} and T_{p1} as shown in figure 3(b), the crystallization activation energies of E_{x1} and E_{p1} have been obtained to be $230\,kJ\,mol^{-1}$ and $246\,kJ\,mol^{-1}$, respectively. It is widely reported that the E_{x1} is related to the nucleation of grains and E_{p1} is attributed to the growth [23, 24]. The relatively high E_{x1} indicates the fine thermal stability of such amorphous alloy against the crystallization when the temperature rises. A larger E_{p1} than E_{x1} was commonly found in most Fe-based nano-crystalline alloys [24, 25]. Also, based on the extended fitting results, the related crystallization temperatures at $400\,K\,min^{-1}$ corresponding to $722\,K$ for T_{x1} and $730\,K$ for T_{p1} have been estimated, providing an important reference for analyzing the kinetics behaviors with rapid heating ($400\,K\,min^{-1}$) during annealing.

3.2. The dependence of magnetic softness on annealing temperature

To investigate the dependence of magnetic softness on the annealing temperature, the as-spun $Fe_{83}Si_4B_8P_{4.3}Cu_{0.7}$ ribbons were annealed at various temperatures of 700–800 K for 10 min with the heating rates of $400\,K\,min^{-1}$ and $10\,K\,min^{-1}$, respectively. The dependence of coercivity on the annealing temperature is shown in figure 4. The lines are guides based on the experimental results for better exhibiting coercivity evolution. Generally, the rapid heating seems necessary for the fine magnetic softness in $Fe_{83}Si_4B_8P_{4.3}Cu_{0.7}$ alloys, and dramatically decreases the coercivity compared with that for slow heating. For the heating rate of $400\,K\,min^{-1}$, it could be found that the coercivity of annealed samples increases first and then decreases followed by a reversal increase and serious deterioration of magnetic softness as the temperature rises, consistent with ones of most Fe-based nano-crystalline alloys [26–28]. The coercivity evolution could be explained by the magnetic exchange coupling between the different phases or magnetic domain regions. A random anisotropy model (RMA) was proposed and commonly applied to explain the dependence of coercivity on the grain size in nano-crystalline alloys through ignoring the effect of the residual amorphous matrix [29]. In fact, the coercivity is dependent on both the distance between α-Fe grains and the grain size of α-Fe in the amorphous matrix. It is reported that the decrease of coercivity of annealed samples for $400\,K\,min^{-1}$ in figure 4 should be mainly attributed to the increase of the crystallization volume fraction (α) and the improvement of magnetic coupling [27], agreeing well with the decrease of residual amorphous trace around 45° in XRD patterns of annealed samples as shown in figure 5(a). The symbols of full circles and open squares in figure 5(a) correspond to α-Fe phase and $Fe_3(B, P)$ phase, respectively. Also, the standard diffraction patterns of α-Fe phase and $Fe_3(B, P)$ phase have been provided. On the other hand, the coercivity of annealed samples is attributed to the grain size of α-Fe phase dispersing in the amorphous matrix. The mean grain size (D) is evaluated by the Scherrer formula from the full width at half maximum of the (110) peak of α-Fe phase in XRD patterns, which is shown in figure 5(b). The guide lines are B-spline curves based on the experimental results to exhibit the evolution of D. As expected, the D increases and then tends to be constant as the annealing temperature rises, consistent with the previous result [30]. Thus, the crystallization of the first stage is almost finished when the annealing temperature with the heating rate of $400\,K\,min^{-1}$ reaches 750 K. A small amount rise of α causes a slight increase of coercivity due to
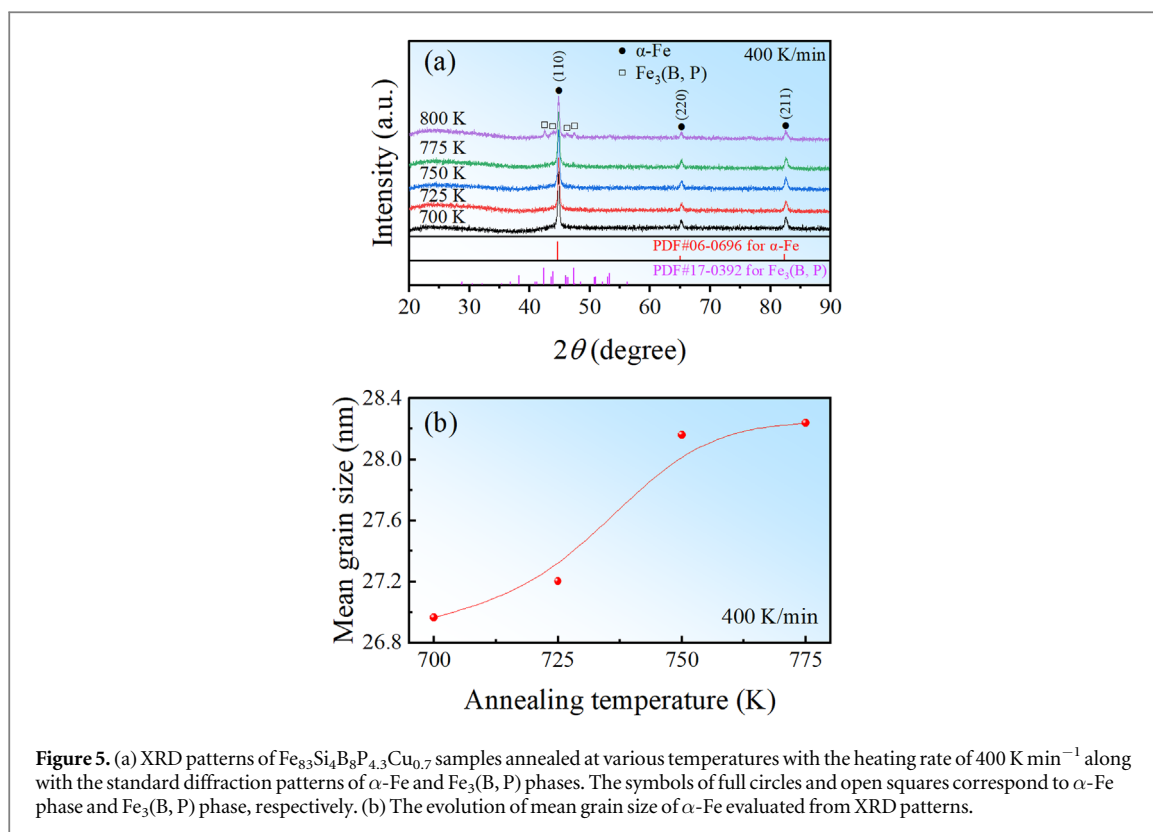
Figure 5. (a) XRD patterns of $Fe_{83}Si_4B_8P_{4.3}Cu_{0.7}$ samples annealed at various temperatures with the heating rate of 400 K min^{-1} along with the standard diffraction patterns of α-Fe and $Fe_3(B, P)$ phases. The symbols of full circles and open squares correspond to α-Fe phase and $Fe_3(B, P)$ phase, respectively. (b) The evolution of mean grain size of α-Fe evaluated from XRD patterns.
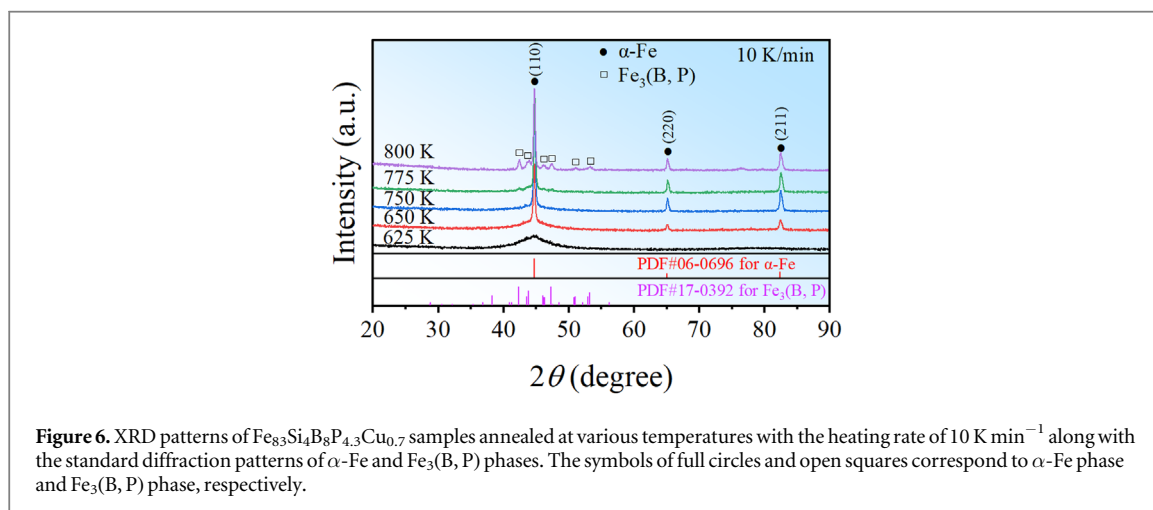
Figure 6. XRD patterns of $Fe_{83}Si_4B_8P_{4.3}Cu_{0.7}$ samples annealed at various temperatures with the heating rate of 10 K min^{-1} along with the standard diffraction patterns of α-Fe and $Fe_3(B, P)$ phases. The symbols of full circles and open squares correspond to α-Fe phase and $Fe_3(B, P)$ phase, respectively.

the large D of α-Fe for samples annealed at 775 K with 400 K min^{-1}. When the annealing temperature reaches 800 K, the appearance of compounds (i.e. $Fe_3(B, P)$) brings a significant deterioration of magnetic softness.

On the other hand, a continuous increase of coercivity with temperature increasing for samples annealed at 10 K min^{-1} is found in figure 4. Figure 6 shows the XRD patterns of samples annealed at various temperatures with 10 K min^{-1}. The amorphous state of the sample after 625 K annealing has been retained, indicating such temperature is too low to trigger the crystallization. It also agrees well with DSC results with the relatively high T_{x1} of 662 K at 10 K min^{-1}. The much low coercivity of the sample annealed at 625 K should be caused by the release of stress in amorphous state accompanied by the formation of homogeneous magnetic coupling regions [18]. Only α-Fe phase appears with the annealing temperature reaching 650 K at 10 K min^{-1}. As the temperature further rises beyond 775 K, a small amount of $Fe_3(B, P)$ phase precipitated from the residual amorphous matrix, causing the severe deterioration of magnetic softness of annealed samples. Thus, the coercivity evolution at 10 K min^{-1} in figure 4 should be dominated by the coursing of α-Fe grains at low temperatures (650–750 K) and the appearance of compounds at high temperatures. These results could help with the further investigation of magnetic properties when the two- and multi-step heating processes are applied during the annealing.
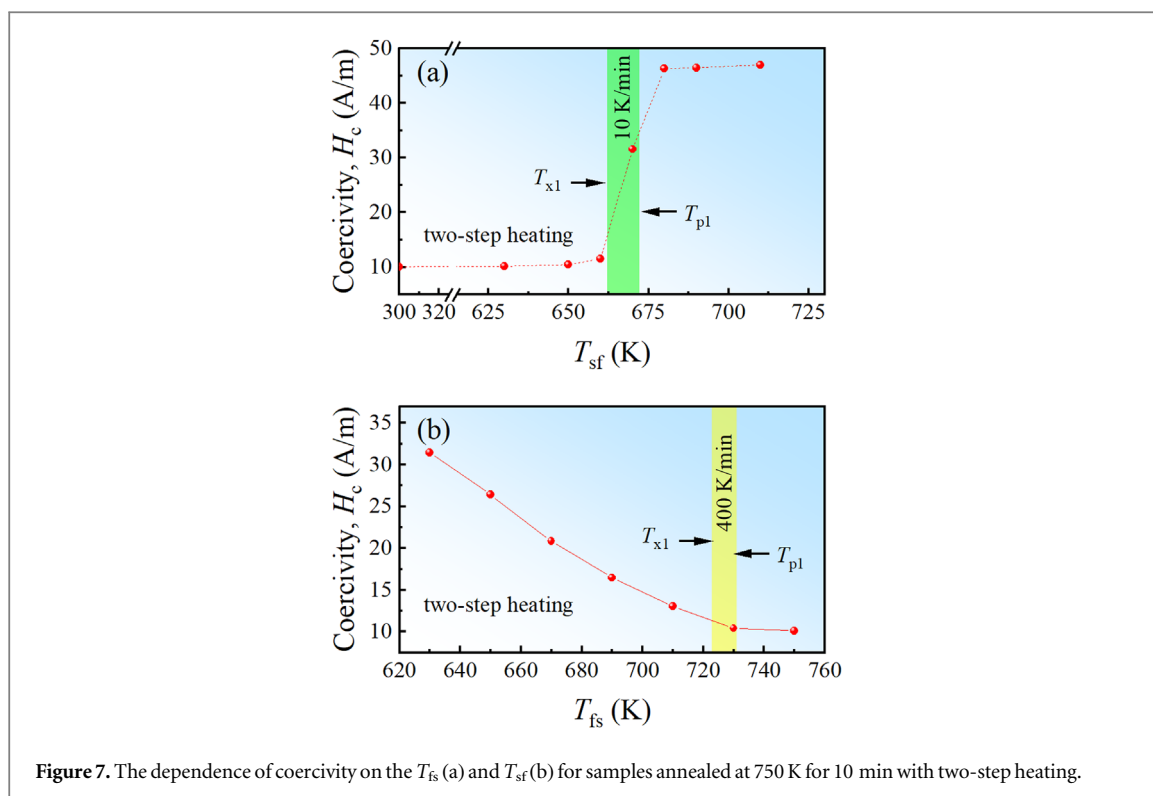
Figure 7. The dependence of coercivity on the T_{fs} (a) and T_{sf} (b) for samples annealed at 750 K for 10 min with two-step heating.

To understand the effect mechanism of heating rate on improving magnetic softness for nano-crystalline alloys, the two-step heating rate has been applied during annealing. As mentioned above, 750 K is sufficient for the relatively complete crystallization of the first stage due to the lowest coercivity of annealed sample with 400 K min^{-1}. Thus, the 750 K is set to be the isothermal target temperature.

3.3. Coercivity evolution of samples annealed with two-step heating

First, the two-step heating from slowing heating to fast heating was applied and the switching temperature is marked to be T_{sf} as introduced in section 2. The dependence of coercivity on T_{sf} for samples annealed at 750 K for 10 min is shown in figure 7(a). The guide lines are B-spline curves based on the experimental results for better exhibiting coercivity evolution for two-step heating. It could be found that the coercivity is unchanged at low T_{sf}. The heating rate seems to hardly affect the crystallization behaviors of as-spun alloy. After the T_{sf} reaches 660 K, the coercivity of annealed samples dramatically increases, indicating the appearance of severe coarsening of α-Fe grains. Compared with the DSC results at 10 K min^{-1}, the crucial temperature of 660 K is slightly lower than the T_{x1} of 662 K. The temperature of deteriorating magnetic softness by low heating mainly ranges from 660 K to 670 K, corresponding to the temperature range between T_{x1} and T_{p1} in DSC curves at 10 K min^{-1}. When the T_{sf} is beyond T_{p1} for 10 K min^{-1}, the high heating rate seems to no longer help with the decrease of coercivity.

For comparison, another series of two-step heating process corresponding to the fast heating to slow heating was also carried out, and the characteristic switching temperature is marked as T_{fs}. The coercivity evolution with T_{fs} increasing is exhibited in figure 7(b). The coercivity of annealed samples declines and the decrement also decreases as the T_{fs} rises. When T_{fs} reaches around 730 K, the rapid heating hardly helps with the decrease of coercivity. A similar tendency also could be observed with the T_{sf} reaching around T_{p1} in DSC curve at 10 K min^{-1} as shown in figure 7(a). Thus, T_{p1} should be a critical temperature to distinguish the nucleation and growth processes of α-Fe phase. In DSC curves, the thermal behavior for the temperature below T_{p1} is dominated by the nucleation process whereas the subsequent stage is mainly dominated by the growth one. The nucleation of α-Fe would be almost finished when the heating temperature reaches T_{p1} at a constant heating rate, causing the hardly changed coercivity values in figure 7. Thus, these results also provided an effective way to study and clarify the characteristic crystallization stages in DSC curves. The improvement of magnetic softness from the high heating rate should mainly focus on the heating stage with the temperature below the T_{p1} of 730 K at 400 K min^{-1}.

As is well-known, the rapid heating is always found effective in decreasing coercivity in most Fe-based nano-crystalline alloys [16, 17]. It is significantly important to link the effective temperature range of rapid heating and magnetic softness of annealed samples along with the thermal behaviors in DSC curves. For further
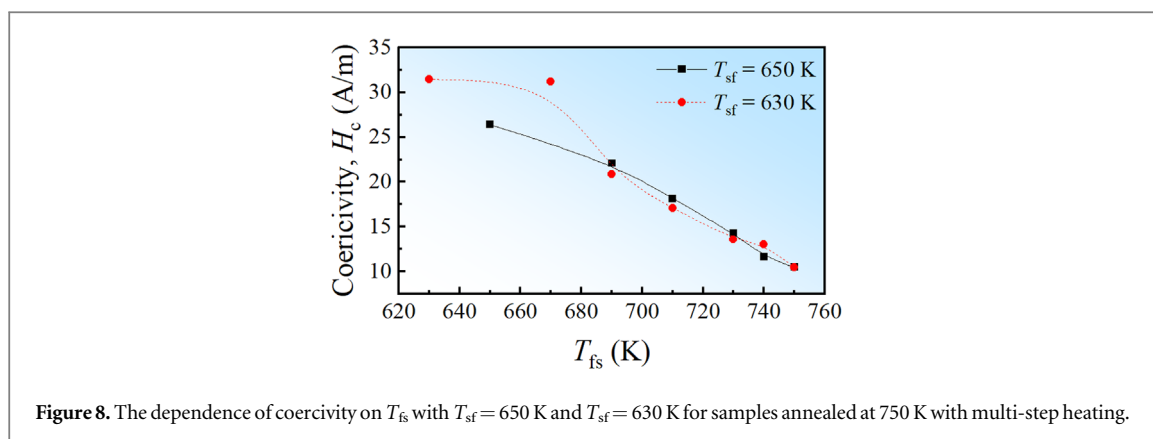
Figure 8. The dependence of coercivity on T_{fs} with $T_{sf} = 650$ K and $T_{sf} = 630$ K for samples annealed at 750 K with multi-step heating.

understanding of the effect of heating rate on coercivity in this study, especially for the onset critical temperature for refinement of magnetic softness, the multi-stage heating was applied during annealing as follows.

3.4. The improvement of magnetic softness from partial rapid heating

As mentioned above, coercivity seriously increases as the T_{sf} ranges from 660 K to 670 K at the heating rate of 10 K min^{-1} [figure 7(a)], corresponding to the approximate temperature range of T_{x1} and T_{p1} of DSC curves, respectively. It is too late to decrease the coercivity through the high heating when the T_{sf} is beyond T_{x1} at 10 K min^{-1}, indicating that the rapid heating plays a significant role around the onset crystallization stage. With T_{fs} rising, the decrement of coercivity decreases and hardly changes after 730 K, consistent with the T_{p1} at 400 K min^{-1} deduced from the Kissinger function. The critical stage of α-Fe gain refinement through rapid heating should begin from the temperature below the T_{x1} for 10 K min^{-1} and finish up around the T_{p1} for 400 K min^{-1}. Thus, the multi-step of slow-fast-slow heating was carried out to investigate the effective temperature range for the decrease of coercivity through the rapid heating.

The coercivity dependence on the T_{fs} for $T_{sf} = 650$ K and 630 K for multi-step heating is shown in figure 8. The guide lines are B-spline curves based on the experimental results to exhibit the coercivity evolution. The study was focused on the necessary rapid heating stage during annealing, which should be important for the fabrication of nana-crystalline alloys in industry. It is found that the coercivity evolution at the relatively high T_{fs} for $T_{sf} = 650$ K is similar to that for $T_{sf} = 630$ K, indicating the lower initial temperature (<650 K) for rapid heating hardly affects the crystallization behaviors and magnetic softness of annealed samples. With the T_{fs} rising for both $T_{sf} = 650$ K and 630 K, the coercivity of annealed samples dramatically decreases and becomes close to the value for the direct rapid heating to 750 K. Ignoring the slight difference of coercivity of samples when the T_{fs} reaches 640 K, the critical stage of rapid heating could be limited in the range from around 650 K to 740 K.

4. Discussion

According to the classical nucleation theory [31], the radius of nucleation seed needs to be above the critical value (r_{crit}) during the crystallization of Fe-based amorphous alloys. Otherwise, the seed would redissolve. Generally, the r_{crit} is much lower than that of finally formed grains, indicating a small amount of crystallization contribution from the nuclei to exothermic behaviors for few grains during heating. The observable exothermic behaviors during the initial stage of crystallization in DSC curves should be contributed by the formation of massive nuclei. Once the nuclei forms, the grain growth would proceed due to its contribution to the decrease of system energy. As the grain becomes larger, it would be surrounded by the B- or P-rich environment and further growth needs long-range diffusion of Fe atoms [32]. As the temperature rises, the ability of atomic rearrangement in amorphous alloys would increase, leading to the accelerated nucleation and growth processes in theory. On the other hand, these two processes would be limited by the supersaturation decrease of Fe in residual amorphous alloy with the crystallinity increasing. Thus, the rates of both nucleation and growth processes increase and then decline with the temperature rising during heating [33].

Due to the protection of metalloid-rich conditions and the necessary long-range diffusion of atoms for the overgrowth of α-Fe grains [32], the low temperatures favor the nucleation and the high ones help with the growth. The increase of the heating rate may highly limit the long-range diffusion ability instead of the short-range one. It also means that the rapid heating severely weakens the growth of grains compared with the nucleation. The effect of the heating rate on nucleation and growth could be sketchily exhibited as shown in figure 9. The improvement of magnetic softness significantly needs to inhibit the overgrowth of α-Fe grains during the nucleation stage. This study has revealed that the nucleation process is almost finished below the T_{p1}
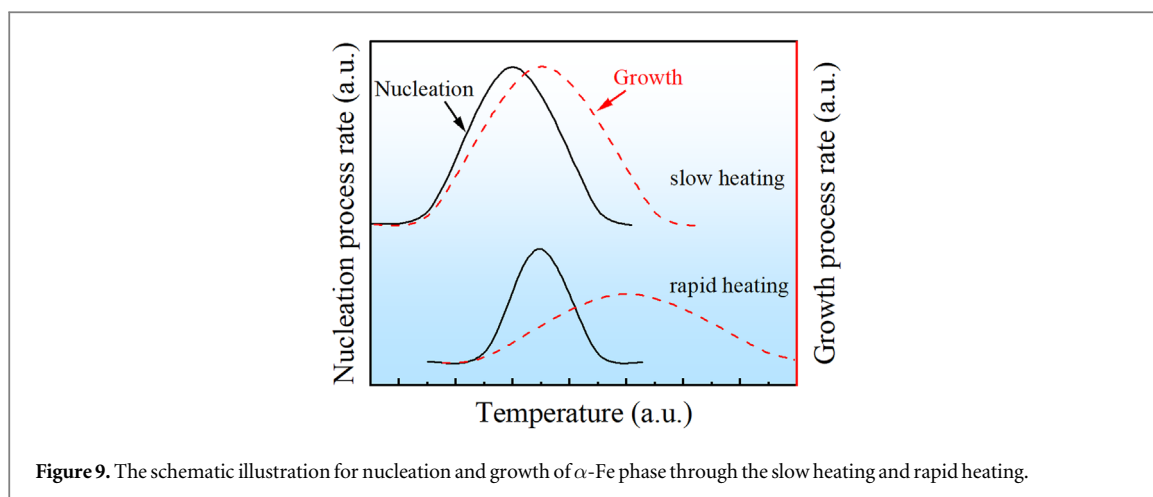
Figure 9. The schematic illustration for nucleation and growth of α-Fe phase through the slow heating and rapid heating.

in DSC curves at a certain heating rate. Thus, the grain refinement could be realized by shortening the time $\Delta t = \Delta T/\beta = (T_{p1} - T_{x1})/\beta$ through the rapid heating. The Δt could be approximately regarded as the growth time before the complete nucleation. It is found that the Δt decreases from 60 s for 10 K min^{-1} to 1.35 s for 400 K min^{-1} in Fe$_{83}$Si$_4$B$_8$P$_{4.3}$Cu$_{0.7}$ alloy.

As mentioned above, E_{x1} and E_{p1} are associated with T_{x1} and T_{p1}, respectively. These related parameters are also dependent on the compositions. With the increase of E_{x1} or the decrease of E_{p1}, the ΔT and Δt of rapid heating would decline compared with that of slow heating. It may imply that the coercivity of annealed samples is more sensitive to the heating rate, or the high heating makes much help to improve the magnetic softness compared with that for slow heating.

With much higher temperature of crystallization than that for many application as devices, Fe-Si-B-P-Cu alloy system with excellent magnetic properties is promising in industry and the heat treatment of these materials should be further improved. The study has determined the necessary temperature range of rapid heating from around T_{x1} of 10 K min^{-1} to T_{p1} at 400 K min^{-1} in Fe$_{83}$Si$_4$B$_8$P$_{4.3}$Cu$_{0.7}$ alloy. Commonly, the key application of soft magnetic nano-crystalline ribbons is the cores of electrical transformers, which are prepared by stacking the as-spun ribbons before the annealing process due to the severe brittleness of as-spun state. It causes the actual difficulty of applying the uniform temperature field for the cores during heating. The heat from external conditions could be hardly controlled during rapid heating and crystallization heat is difficult to be dispersed in time. As a result, it seriously limited the fabrication of large-size soft magnetic devices as mentioned above. Thus, determining and reducing the necessary temperature range of rapid heating should be important. In this study, it is revealed that the partial rapid heating could also make a similar improvement of coercivity of Fe-based nano-crystalline alloys and the effective temperature range of a high heating rate of 400 K min^{-1} for Fe$_{83}$Si$_4$B$_8$P$_{4.3}$Cu$_{0.7}$ alloy has been obtained to be from around 650 K to 740 K. Less necessary temperature range through the high heating rate could also be realized by the compositional adjustment, which should further favor the controllable heat treatment for large-size devices. Based on these results, coatings with exothermic process at appropriate temperatures for ribbons are also worth trying to improve the heating process in future.

5. Conclusion

In this study, the crystallization behaviors of Fe$_{83}$Si$_4$B$_8$P$_{4.3}$Cu$_{0.7}$ amorphous alloy were investigated in detail. The onset crystallization and peak temperatures of the first stage at 400 K min^{-1} are estimated to be 722 K and 730 K based on the Kissinger model. When the temperature is below the T_{p1} in DSC curves during heating, the crystallization of amorphous alloys should be mainly dominated by the nucleation process of α-Fe phase. It also means that the nucleation process is almost finished when the temperature reaches T_{p1}, whereas the subsequent crystallization behavior is mainly contributed by the growth process. As a result, E_{p1} seems to be strongly related to the grain growth of α-Fe. The critical temperature range of high heating rate (400 K min^{-1}) for improving magnetic softness has been determined from around 650 K to 740 K. The multi-step heating is found to be an effective strategy for the investigation of the crystallization mechanism of amorphous alloys. These results could also substantively help with the heat treatment for fabricating high-performance soft magnetic alloys with the necessary rapid heating in industry.

Acknowledgments

Data availability statement

The data that support the findings of this study are available upon reasonable request from the authors.

Conflict of interest

The authors declare no potential conflicts of interest.

CRediT authorship contribution statement

Ziyan Hao: Investigation, Data curation, Writing—Original draft. **Linzhuo Wei:** Investigation. **Yuanfei Cai:** Investigation. **Yaocen Wang:** Conceptualization, Formal analysis. **Mingliang Xiang:** Investigation. **Fang Chen:** Investigation. **Yan Zhang:** Supervision, Writing—Review & Editing. **Nikolai S. Perov:** Investigation. **Chongde Cao:** Supervision, Writing—Review & Editing.

ORCID iDs

Yaocen Wang ⓘ https://orcid.org/0000-0002-9773-737X

References

[1] Ouyang G Y *et al* 2021 Effect of solidification cooling rates on microstructures and physical properties of Fe-6.5%Si alloys *Acta Mater.* **205** 116575
[2] Shokrollahi H and Janghorban K 2007 Influence of additives on the magnetic properties, microstructure and densification of Mn-Zn soft ferrites *Mater. Sci. Eng. B* **141** 91–107
[3] Parra C, Perea C and Bolivar F J 2019 Effect of cobalt addition on the microstructural evolution, thermal stability and magnetic properties of Fe-based amorphous alloys *Vaccum* **169** 108911
[4] Takada Y, Abe M, Masuda S and Inagaki J 1988 Commercial scale production of Fe-6.5 wt.% Si sheet and its magnetic properties *J. Appl. Phys.* **64** 5367–9
[5] Wang J F, Li R, Hua N B, Huang L and Zhang T 2011 Ternary Fe-P-C bulk metallic glass with good soft-magnetic and mechanial properties *Scripta Mater.* **65** 536–9
[6] Makino A, Kubota T, Chang C, Makabe M and Inoue A 2007 FeSiBP bulk metallic glasses with unusual combination of high magnetization and high glass-forming ability *Mater. Trans.* **48** 3024–7
[7] Zhou J F, You J H and Qiu K Q 2022 Advances in Fe-based amorphous/nanocrystlline alloys *J. Appl. Phys.* **132** 040702
[8] Liu T, Wang A N, Zhao C L, Yue S G, Wang X M and Liu C T 2019 Compositional design and crystallization mechanism of high Bs nanocrystalline alloys *Mater. Res. Bull.* **112** 323–30
[9] Li Z, Yao K F, Liu C T and Wang S 2022 Effect of annealing on the magnetic properties of FeCoNiCuNbSiB soft magnetic alloys *Front. Mater.* **8** 805609
[10] Herzer G 2013 Modern soft magnets: amorphous and nanocrystalline materials *Acta Mater.* **61** 718–34
[11] Yoshizawa Y, Oguma S and Yamauchi K 1988 New Fe-based soft magnetic alloys composed of ultrafine grain structure *J. Appl. Phys.* **64** 6044–6
[12] Suzuki K, Makino A, Inoue A and Masumoto T 1991 Soft magnetic-properties of nanocrystalline bcc Fe-Zr-B and Fe-M-B-Cu (M = transition-metal) alloys with high saturation magnetization *J. Appl. Phys.* **70** 6232–7
[13] Xie L, Liu T, He A N, Li Q, Gao Z K, Wang A D, Chang C T, Wang X M and Liu C T 2018 High Bs Fe-based nanocrystalline alloy with high impurity tolerance *J. Mater. Sci.* **53** 1437–46
[14] Liu T, He A N, Wang A D, Wang X M, Zhang H and Ni H W 2022 Stabilizing Fe-based nanocrystalline alloys via a high-entropy strategy *J. Alloys Compd.* **896** 163138
[15] Makino A, Men H, Kubota T, Yubuta K and Inoue A 2009 New excellent soft magnetic FeSiBPCu nanocrystallized alloys with high Bs of 1.9 T from nanohetero-amorphous phase *IEEE Trans. Magn.* **45** 4302–5
[16] Parsons R, Zang B, Onodera K, Kishimoto H, Shoji T, Kato A and Suzuki K 2018 Nano-crystallisation and magnetic softening in Fe-B binary alloys induced by ultra-rapid heating *J. Phys. D Appl. Phys.* **51** 415001
[17] Zang B, Parsons R, Onodera K, Kishimoto H, Kato A, Liu A C Y and Suzuki K 2017 Effect of heating rate during primary crystallization on soft magnetic properties of melt-spun Fe-B alloys *Scr. Mater.* **132** 68–72
[18] Nomura Y, Uzuhashi J, Tomita T, Takahashi T, Kuwata H, Abe T, Ohkubo T and Hono K 2021 Heating rate dependence of coercivity and microstructure of Fe-B-P-Cu nanocrystalline soft magnetic materials *J. Alloys Compd.* **859** 157832

[19] Ohta M and Hasegawa R 2017 Soft magnetic properties of magnetic cores assembled with a high Bs Fe-Based nanocrystalline alloy *IEEE Trans. Magn.* **53** 2000205

[20] Jiang L X, Zhang Y, Tong X, Suzuki T and Makino A 2019 Unique influence of heating rate on the magnetic softness of $Fe_{81.5}Si_{0.5}B_{4.5}P_{11}Cu_{0.5}C_2$ nanocrystalline alloy *J. Magn. Magn. Mater.* **47** 148–52

[21] Pradeep K G, Herzer G, Choi P and Raabe D 2014 Atom probe tomography study of ultrahigh nanocrystallization rates in FeSiNbBCu soft magnetic amorphous alloys on rapid annealing *Acta Mater.* **68** 295–309

[22] Kissinger H E 1957 Reaction kinetics in differential thermal analysis *Anal. Chem.* **29** 1702–6

[23] Qin F X, Zhang H F, Ding B Z and Hu Z Q 2004 Nanocrystallization kinetics of Ni-based bulk amorphous alloy *Intermetallics* **12** 1197–203

[24] Xie Z Y, Wang Z, Han Y and Han F F 2017 Influence of Ge on crystallization kinetics, microstructure and high-temperature magnetic properties of Si-rich nanocrystalline FeAlSiBCuNbGe alloy *J. Non-Cryst. Solids* **463** 1–5

[25] Fan X D and Shen B L 2015 Crystallization behavior and magnetic properties in high Fe content FeBCSiCu alloy system *J. Magn. Magn. Mater.* **385** 277–81

[26] Shen N N, Dou Z X, Li Y L, Lv K, Wu Y D, Li F S and Hui X D 2021 Effect of Fe content on crystallization behavior and soft magnetic properties in FINEMET-type alloys *Mater. Lett.* **305** 130759

[27] Xu J, Yang Y Z, Yan Q S, Hou F T, Fan C F, Wang G T and Luo T 2020 Effects of the substitution of Si by P on crystallization behavior, soft magnetic properties and bending ductility of FeSiBCuPC alloys *J. Alloys Compd.* **816** 152534

[28] Zhu Q K, Chen Z, Zhang S L, Li Q S, Jiang Y, Wu P X and Zhang K W 2019 Crystallization progress and soft magnetic properties of FeGaBNbCu alloys *J. Magn. Magn. Mater.* **475** 88–92

[29] Herzer G 1990 Grain size dependence of coercivity and permeability in nanocrystalline ferromagnets *IEEE Trans. Magn.* **26** 1397–402

[30] Wang Y C, Zhang Y, Takeuchi A, Makino A and Kawazoe Y 2016 Investigation on the crystallization mechanism difference between FINEMET® and NANOMET® type Fe-based soft magnetic amorphous alloys *J. Appl. Phys.* **120** 145102

[31] Thanh N T K, Maclean N and Mahiddine S 2014 Mechanism of nucleation and growth of nanoparticles in silution *Chem. Rev.* **14** 7610–30

[32] Liu T, Li F C, Wang A D, Xie L, He Q F, Luan J H, He A N, Wang X M, Liu C T and Yang Y 2019 High performance Fe-based nanocrystalline alloys with excellent thermal stability *J. Alloys Compd.* **776** 606–13

[33] Man Z, Fa Y, Yao L J, Tao P, Jian Z Y and Chang F E 2018 The influence of annealing on the structural and soft magnetic properties of $(Fe_{0.4}Co_{0.6})Nb_3B_{18}$ nanocrystalline alloys *Materials* **11** 2171